Doi: 10.4149/gpb_2022054

Circ_0001498 contributes to lipopolysaccharide-induced lung cell apoptosis and inflammation in sepsis-related acute lung injury *via* upregulating SOX6 by interacting with miR-574-5p

Wei Hu[1], Qin Wang[2], Zhichun Luo[1], Yaqiong Shi[1], Liangping Zhang[1], Zhijun Zhang[1], Jianlin Liu[1] and Kelan Liu[1]

[1] *Intensive care unit, Liyang People's Hospital, Liyang, China*
[2] *Department of Respiratory and Critical Care Medicine, Jinling Hospital, Nanjing, China*

Abstract. Circular RNAs (circRNAs) have important regulation in in sepsis-related acute lung injury (ALI). Circ_0001498 was significantly overexpressed in sepsis-induced acute respiratory distress syndrome. The aims of this study were to explore role and mechanism of circ_0001498 in lipopolysaccharide (LPS)-treated WI-38 cells. Human samples were collected from 56 sepsis patients and 46 healthy volunteers at Liyang People's Hospital. Circ_0001498, microRNA-574-5p (miR-574-5p) or sex-determining region Y-related high-mobility-group box 6 (SOX6) levels were detected *via* reverse transcription-quantitative polymerase chain reaction assay. Cell viability was determined through Cell Counting Kit-8 assay. Apoptosis rate was examined by flow cytometry. Western blot was used for measurement of proteins. Inflammatory cytokines were detected *via* enzyme-linked immunosorbent assay. Target relation was analyzed *via* dual-luciferase reporter assay and RNA immunoprecipitation (RIP) assay. Circ_0001498 was overexpressed in sepsis-related ALI patients and LPS-treated WI-38 cells. Silencing circ_0001498 reduced LPS-induced cell apoptosis and inflammation. Circ_0001498 interacted with miR-574-5p. The regulation of circ_0001498 knockdown was abolished by miR-574-5p inhibitor. Furthermore, miR-574-5p directly targeted SOX6 and circ_0001498 upregulated SOX6 *via* targeting miR-574-5p. Overexpression of miR-574-5p alleviated LPS-induced cell injury by downregulating SOX6. This research identified that circ_0001498 facilitated sepsis-related ALI progression by targeting miR-574-5p to upregulate SOX6.

Key words: Circ_0001498 — Sepsis-induced acute lung injury — miR-574-5p — SOX6

Introduction

Acute lung injury (ALI) is a heterogeneous pulmonary disorder of respiratory system and it can be induced by sepsis, which results in serve effect on human health with high morbidity and mortality (Xu H et al. 2021). Sepsis-induced ALI exhibits lung cell apoptosis and systemic inflammatory response (Sadowitz et al. 2011). Lipopolysaccharide (LPS) is commonly used to induce lung inflammation to mimic sepsis-related ALI (Lennon and Singleton 2011). RNA molecules have been found to act as important regulators in sepsis-induced organ dysfunctions (Brandenburger et al. 2018; Wang W et al. 2021). It is necessary to explore the function and molecular mechanism of noncoding RNAs (ncRNAs) in sepsis-induced ALI.

Circular RNAs (circRNAs) are stable and conserved RNAs produced from non-classical back-splicing (Qu et al. 2015). CircRNAs are reported to play essential roles in various

Correspondence to: Kelan Liu, Intensive care unit, Liyang People's Hospital, No. 70, Jianshe West Road, Liyang 213300, China
E-mail: lkl19830012@163.com

kinds of human diseases, including sepsis and associated complications (Beltran-Garcia et al. 2020; Ghafouri-Fard et al. 2021). A recent expression file of circRNAs showed that circ_0001498 was significantly overexpressed in sepsis-induced acute respiratory distress syndrome (Guo et al. 2021). The function of circ_0001498 in sepsis-induced ALI is not clear.

CircRNAs are known to serve as microRNA (miRNA) sponges, consequently leading to expression changes of downstream genes (Panda 2018). Sun et al. (2020) stated that miR-574-5p level was reduced in sepsis patients and miR-574-5p relieved LPS-induced lung cell apoptosis. Zhang et al. (2021) disclosed that abnormal expression of sex-determining region Y-related high-mobility-group box 6 (SOX6) was detected in septic lung tissues and miR-499-5p attenuated lung injury through downregulating SOX6. Target correlation of miR-574-5p and SOX6 remains unclear and association of circ_0001498 with miR-574-5p/SOX6 is still to be investigated.

Circ_0001498 was assumed as a miRNA sponge for miR-574-5p and SOX6 was assumed as a target for miR-574-5p. Moreover, circ_0001498 was hypothesized to interact with miR-574-5p to regulate SOX6 expression. The objective of this research was to uncover functional mechanism of circ_0001498 in sepsis-related ALI. Interaction between circ_0001498 or SOX6 and miR-574-5p was affirmed in this study.

Materials and Methods

Serum samples

56 sepsis patients were diagnosed as ALI at Liyang People's Hospital, and 2 ml bloods were centrifugated with a speed of 1200 rpm for 10 min. In addition, blood samples were collected from 46 healthy volunteers at Liyang People's Hospital. The supernatant serums of healthy group ($n = 46$) and sepsis group ($n = 56$) were preserved at −80°C. Baseline characteristics of the subjects were shown in Table 1. All procedures were authorized by Ethics Committee of Liyang People's Hospital.

Table 1. Baseline characteristics of the subjects from collected samples

Parameters	Healthy ($n = 46$)	Sepsis ($n = 56$)
Age (years)	57.61 ± 8.62	58.12 ± 9.22
Male/Female	25/21	30/26
BMI (kg/m^2)	23.22 ± 0.54	22.34 ± 0.82
APACHE II score	–	20.61 ± 4.91
LIPS	–	8.57 ± 1.32

Data are presented as mean ± SD. BMI, body mass index; APACHE, acute physiology and chronic health evaluation; LIPS, lung injury prediction score.

Sepsis-induced ALI cell model

Human embryonic lung fibroblasts (WI-38; BioVector NTCC Inc., Beijing, China) were cultured with Dulbecco's modified eagle medium with supplement of 10% fetal bovine serum and 1% antibiotic solution in a 5% CO_2 + 37°C incubator. These reagents for cell culture were bought from Gibco (Carlsbad, CA, USA). To establish sepsis-induced ALI cell model, 10 ng/ml LPS (Sigma, St. Louis, MO, USA) treatment for 48 h was used to stimulate inflammatory response in WT-38 cells. In addition, WT-38 cells in control group were treated with 10 ng/ml phosphate buffer solution (PBS; Gibco).

Cell transfection

Small interfering RNA for circ_0001498 (si-circ_0001498#1, si-circ_0001498#2) and negative control (si-NC), mimic targeting miR-574-5p (miR-574-5p) and matched NC (miR-NC), inhibitor targeting miR-574-5p (anti-miR-574-5p) and corresponding NC (anti-miR-NC), pcDNA-SOX6 (SOX6) and pcDNA expression vector (vector) were synthesized and purchased from RIBOBIO (Guangzhou, China) and GENESEED (Guangzhou, China). These RANs or vectors were diluted with Opti-MEM® Reduced Serum Medium (Gibco) and mixed with Lipofectamine™ 3000 reagent (Invitrogen, Carlsbad, CA, USA), then transfected to WT-38 cells and incubated at 37°C.

Table 2. Primer sequences for RT-qPCR

Name	Primer sequences (5'–3')	
circ_0001498	F:	TCCTTCCTTGGAATCTTGTGAAG
	R:	TTTCCCCTGTCTGGGCATTC
WDR41	F:	CAGGGACTGGCCGAGAAATC
	R:	TTTCCCCTGTCTGGGCATTC
miR-574-5p	F:	GCGGCTGAGTGTGTGTGTGT
	R:	CTCAACTGGTGTCGTGGAGT
SOX6	F:	TGGGACAGCGTTCTGTCATC
	R:	CACATCGGCAAGACTCCCTT
GAPDH	F:	GACAGTCAGCCGCATCTTCT
	R:	GCGCCCAATACGACCAAATC
U6	F:	CTCGCTTCGGCAGCACA
	R:	AACGCTTCACGAATTTGCGT

F, forward; R, reverse.

Reverse transcription-quantitative polymerase chain reaction (RT-qPCR) assay

After RNA extraction from serums and cells by TRI Reagent® (Sigma), the complementary DNA (cDNA) was obtained by ReadyScript® cDNA Synthesis Mix (Sigma) to reversely transcribe total RNA. Then, SYBR® Green Quantitative RT-qPCR Kit (Sigma) was used for preparation of quantitative reaction. The specific primers in Table 2 were synthesized by Sangon (Shanghai, China). Data were analyzed to calculate relative expression *via* the $2^{-\Delta\Delta Ct}$ method (Livak and Schmittgen 2001). Level standardization was carried out by U6 or glyceraldehyde-phosphate dehydrogenase (GAPDH). After total RNA was digested with 5 U/μg RNase R (GENESEED) and WT-38 cells were incubated with 2 mg/ml actinomycin D (Sigma), RT-qPCR was exploited for circ_0001498 or WDR41 stability analysis.

Cell Counting Kit-8 (CCK-8) assay

Cell viability was detected by CCK-8 for quantification of viable cells (Sigma), as *per* manufacturer's directions. In brief, WT-38 cells in 96-well plates were pipetted with 10 μl/well CCK-8 solution. After incubation for 2 h, the absorbance of each well was tested at 450 nm under a microplate reader. Cell viability was expressed the percentage of viable cells in total cells.

Flow cytometry

Apoptotic cells were examined using Annexin V-FITC Apoptosis Detection Kit (Sigma). 1×10^6 WT-38 cells were washed in PBS twice and resuspended with 1×Binding Buffer, then cell suspension was added with 5 μl Annexin V-fluorescein isothiocyanate (Annexin V-FITC) and 10 μl propidium iodide (PI). Tubes were protected from light and incubated for 10 min, then cell fluorescence was immediately determined by the flow cytometer (BD Biosciences, San Diego, CA, USA). Annexin V-FITC alone stained cells were counted as early apoptotic cells, while cells with Annexin V-FITC and PI double-staining were counted as late apoptotic cells. Apoptosis rate = (early apoptotic cells + late apoptotic cells)/total cells × 100%.

Western blot

BCA Protein Assay Kit (Sigma) was employed for detection of concentration after total proteins were extracted using Radioimmunoprecipitation assay buffer (Sigma). As previously reported (Zhong et al. 2021; Zhou et al. 2021), Western blot was performed with 50 μg proteins of each sample. The used primary antibodies were commercially provided by Abcam (Cambridge, MA, USA): B-cell lymphoma-2 (Bcl-2; ab59348, 1:1000), cleaved caspase 3 (ab32042, 1:1000), cleaved poly-ADP-ribose polymerase (cleaved PARP; ab32064, 1:1000), SOX6 (ab64946, 1:1000), GAPDH (ab128915, 1:2000). After IgG H&L (HRP) secondary antibody (Abcam, ab205718, 1:5000) was incubated for 60 min, protein blot visualization was conducted through Electrochemiluminescence (ECL) Ultra Western HRP Substrate (Sigma) and protein expression quantification *via* ImageJ software (NIH, Bethesda, MD, USA).

Enzyme-linked immunosorbent assay (ELISA)

Cell supernatants were collected after transfection for 48 h. Tumor necrosis factor-alpha (TNF-α), interleukin-1beta (IL-1β) and interleukin-6 (IL-6) were measured through Human TNF-α/IL-1β/IL-6 ELISA Kit. The operating steps were following instruction books of Sangon. The optical density values were read at 450 nm and concentrations (pg/ml) were calculated according to standard curves.

Dual-luciferase reporter assay

Circ_0001498 and 3'UTR of SOX6 sequences (containing miR-574-5p binding sites) were cloned into pmirGLO (Promega, Madison, WI, USA) to construct wild-type (WT) vectors circ_0001498-WT and SOX6 3'UTR-WT. Then, mutant-type (MUT) vectors circ_0001498-MUT and SOX6 3'UTR-MUT (with mutated miR-574-5p binding sites) were constructed as negative controls. WT-38 cells were performed with co-transfection of luciferase plasmid and mimic (miR-574-5p or miR-NC), then cell incubation was at 37°C for 48 h and activity analysis of luciferase was implemented through Dual-Luciferase Reporter System Promega).

RNA immunoprecipitation (RIP) assay

Circ_0001498 and miR-574-5p binding was analyzed *via* Magna RIP RNA-Binding Protein Immunoprecipitation Kit (Millipore, Billerica, MA, USA). Briefly, Protein A magnetic beads coated with antibody against immunoglobulin G (IgG) or Argonaute-2 (AGO2) were incubated to WT-38 cells at 4°C overnight. Subsequently, total RNA was isolated and RT-qPCR was performed for quantification of circ_0001498 or miR-574-5p.

Statistical analysis

Data were displayed as mean ± standard deviation, then data analysis was administrated using SPSS 22.0 (SPSS Inc., Chicago, IL, USA). Additionally, Pearson's correlation

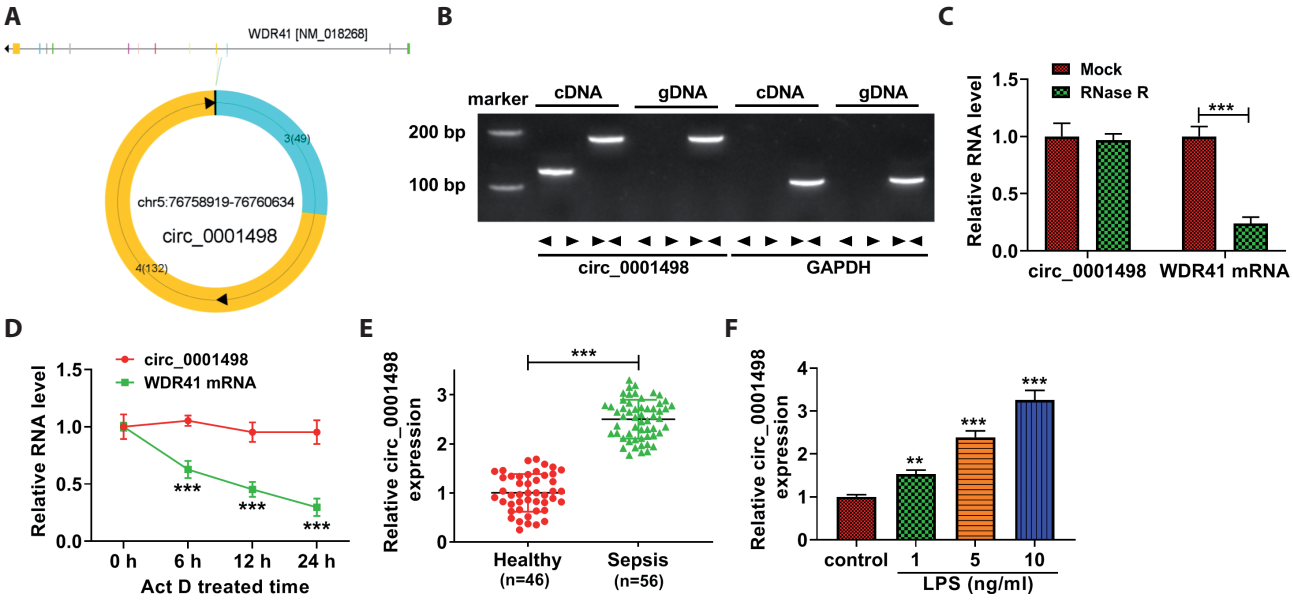

Figure 1. Circ_0001498 expression was upregulated in sepsis-induced ALI patients and LPS-treated WI-38 cells. **A.** Circular structure of circ_0001498. **B.** CircRNA identification of circ_0001498 by gel electrophoresis. WDR41 and circ_0001498 levels were examined by RT-qPCR after RNase R digestion (**C**) or actinomycin D treatment (**D**). **E.** Circ_0001498 expression detection was performed by RT-qPCR in serums of healthy controls and sepsis patients. **F.** RT-qPCR was used to determine circ_0001498 level in control group and LPS treatment groups (1, 5 and 10 ng/ml). ** $p < 0.01$, *** $p < 0.001$.

coefficient was conducted to analyze the linear relations. Student's *t*-test or analysis of variance (ANOVA) followed by Tukey's test was used to evaluate whether difference was significant ($p < 0.05$).

Results

Circ_0001498 expression was upregulated in sepsis-induced ALI patients and LPS-treated WI-38 cells

Circ_0001498 is produced by back-splicing of exon 3 to 4 of WD-repeat protein 41 (WDR41) in chr5: 76758919-76760634 (Fig. 1A). Quantification in cells was conducted using RT-qPCR. Gel electrophoresis by divergent primers suggested that circ_0001498 existed in cDNA but not genomic DNA (gDNA), while linear GAPDH was detected in cDNA and gDNA (Fig. 1B). Circ_0001498 exhibited high stability to protect against RNase R digestion, but WDR41 was degraded by RNase R in WI-38 cells (Fig. 1C). In addition, circ_0001498 was more stable than WDR41 after cell incubation with Actinomycin D (Fig. 1D). The results of RT-qPCR showed that circ_0001498 was highly expressed in sepsis patients relative to healthy controls (Fig. 1E), as well as in LPS-treated WI-38 cells compared with control cells (Fig. 1F). LPS treatment with 10 ng/ml for 24 h was used for further experiments.

Circ_0001498 downregulation protected WI-38 cells against LPS-induced apoptosis and inflammation

The siRNA was used to knock down the expression of circ_0001498, and RT-qPCR data demonstrated that the inhibiting effect of si-circ_0001498#1 or si-circ_0001498#2 was eminent (Fig. 2A). The subsequent assays were performed using si-circ_0001498#1 with more significant difference. Also, level upregulation of circ_0001498 by LPS has been attenuated by si-circ_0001498#1 (Fig. 2B). LPS treatment suppressed cell viability (Fig. 2C) and accelerated cell apoptosis (Fig. 2D), whereas these influences were relieved after transfection of si-circ_0001498#1. Then, protein markers associated with cell apoptosis were examined using Western blot. Knockdown of circ_0001498 obviously counteracted the LPS-induced downregulation of Bcl-2 protein expression and upregulation of cleaved caspase 3 or cleaved PARP protein level (Fig. 2E). ELISA showed that LPS reduced concentrations of TNF-α, IL-β and IL-6, while si-circ_0001498#1 reversed these changes (Fig. 2F). LPS-induced WI-38 cell injury was ameliorated after circ_0001498 downregulation.

Circ_0001498 targeted miR-574-5p

Circinteractome (https://circinteractome.nia.nih.gov/) predicted that there was one binding region between

circ_0001498 and miR-574-5p sequences (Fig. 3A). Transfection of miR-574-5p significantly induced overexpression of miR-574-5p in WI-38 cells (Fig. 3B). Luciferase activity was inhibited by co-transfection with circ_0001498-WT and miR-574-5p, but no difference was noticed after co-transfection of circ_0001498-MUT and miR-574-5p (Fig. 3C). Circ_0001498 and miR-574-5p levels were increased in AGO2 group relative to IgG group, which suggested that circ_0001498 interacted with miR-574-5p in AGO2 protein (Fig. 3D). The miR-574-5p expression was reduced in serums of sepsis patients contrasted to healthy controls (Fig. 3E). Pearson's correlation coefficient analysis manifested that circ_0001498 was negatively related to miR-574-5p ($r = -0.491$, $p = 0.001$) in serum samples of sepsis group (Fig. 3F). Also, miR-574-5p downregulation was detected in LPS treatment groups compared with control group of WI-38 cells (Fig. 3G). Interestingly, miR-574-5p was upregulated after transfection with si-circ_0001498#1 or si-circ_0001498#2 (Fig. 3H). Altogether, circ_0001498 directly interacted with miR-574-5p.

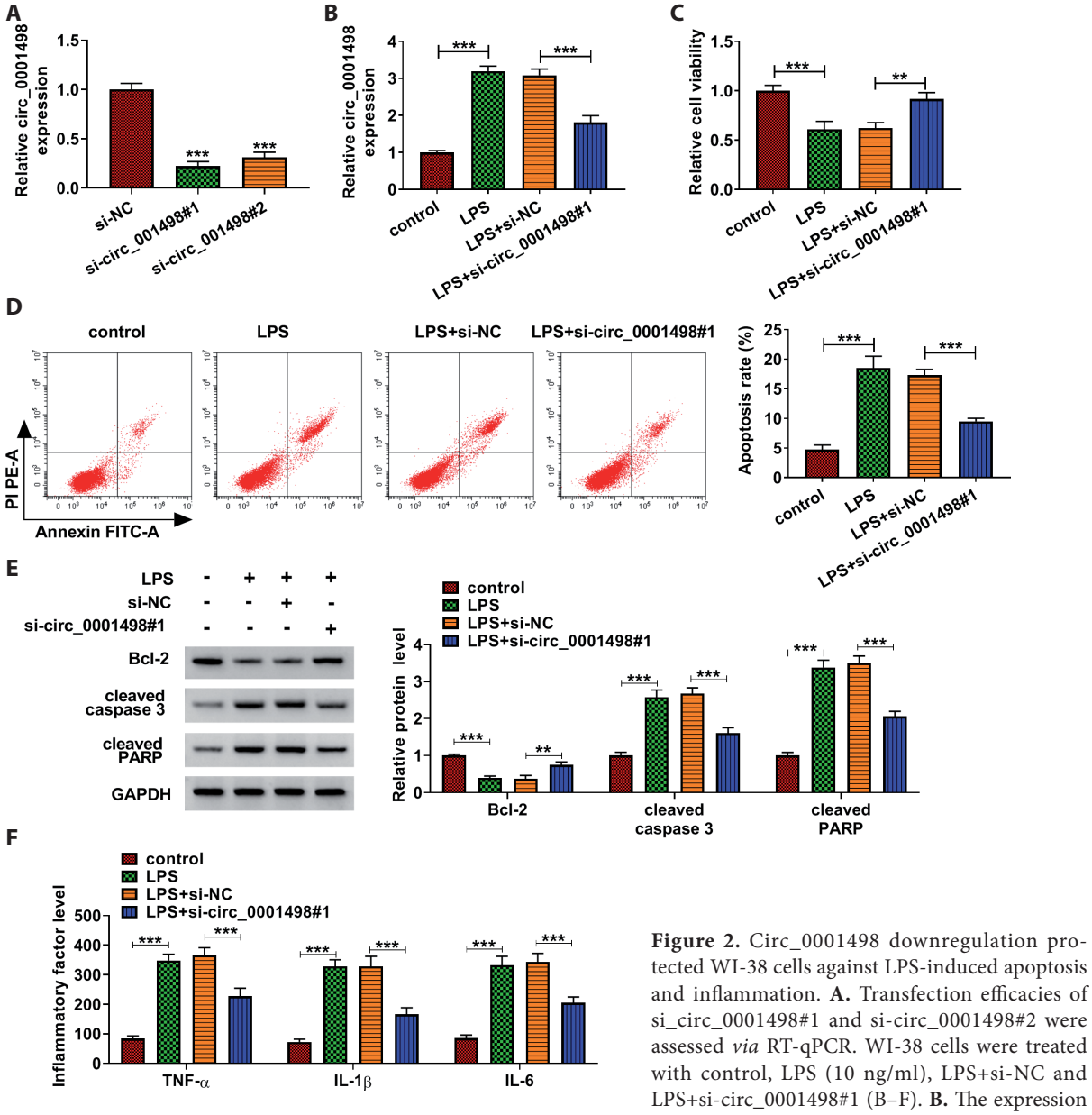

Figure 2. Circ_0001498 downregulation protected WI-38 cells against LPS-induced apoptosis and inflammation. **A.** Transfection efficacies of si_circ_0001498#1 and si-circ_0001498#2 were assessed *via* RT-qPCR. WI-38 cells were treated with control, LPS (10 ng/ml), LPS+si-NC and LPS+si-circ_0001498#1 (B–F). **B.** The expression of circ_0001498 was assayed using RT-qPCR. **C.** Cell viability was detected by CCK-8 assay. **D.** The apoptosis rate was examined through flow cytometry. **E.** Apoptosis-related proteins were determined *via* Western blot. **F.** TNF-α, IL-β and IL-6 concentrations were measured by ELISA. ** $p < 0.01$, *** $p < 0.001$.

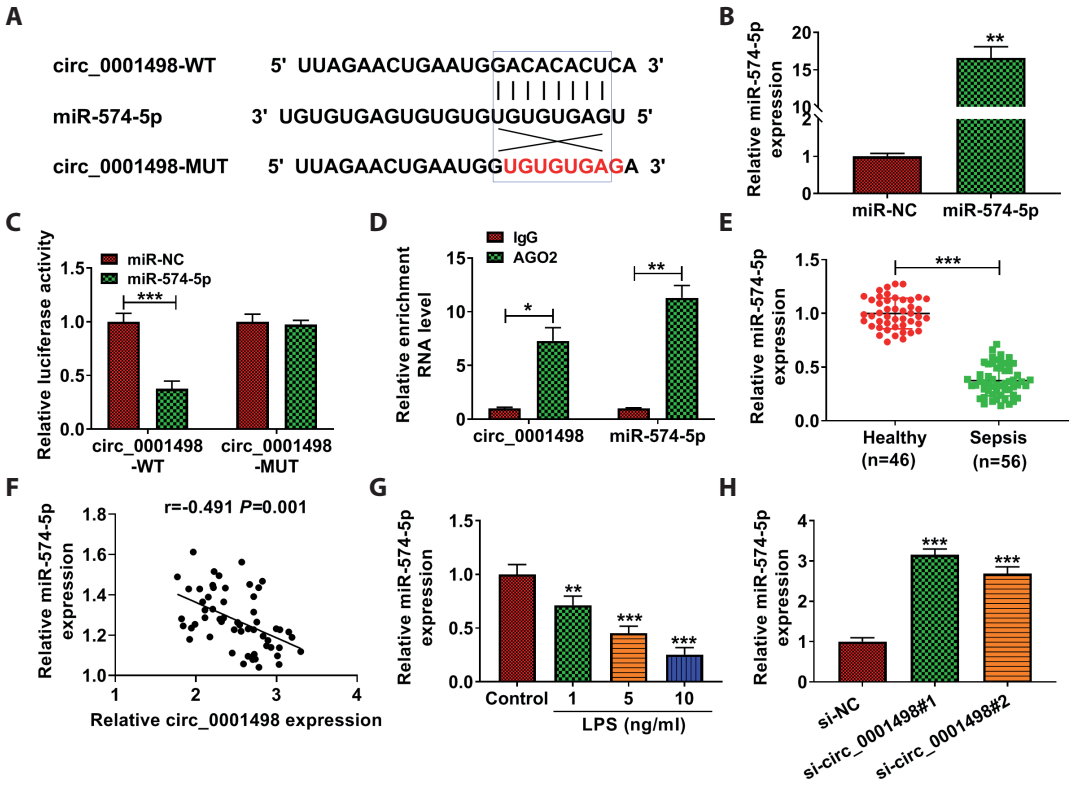

Figure 3. Circ_0001498 targeted miR-574-5p. **A.** Circinteractome was used for site analysis between circ_0001498 and miR-574-5p sequences. **B.** RT-qPCR was applied for miR-574-5p quantification after WI-38 cells were transfected with miR-NC and miR-574-5p. Dual-luciferase reporter assay (**C**) and RIP assay (**D**) were performed to validate binding between circ_0001498 and miR-574-5p. **E.** The miR-574-5p expression was measured by RT-qPCR in sepsis and healthy groups. **F.** Linear relation between circ_0001498 and miR-574-5p was analyzed by Pearson's correlation coefficient in serum samples of sepsis patients. **G.** RT-qPCR was used to assay miR-574-5p level in LPS-treated WI-38 cells. **H.** The miR-574-5p level detection was conducted by RT-qPCR after transfection of si-circ_0001498#1 or si-circ_0001498#2. * $p < 0.05$, ** $p < 0.01$, *** $p < 0.001$.

Inhibition of miR-574-5p abolished the function of circ_0001498 knockdown in LPS-treated WI-38 cells

RT-qPCR displayed that miR-574-5p was downregulated in anti-miR-574-5p group relative to anti-miR-NC group (Fig. 4A). In addition, si-circ_0001498#1-mediated expression elevation of miR-574-5p was offset by anti-miR-574-5p in WI-38 cells (Fig. 4B). These effects of si-circ_0001498#1 on cell viability (Fig. 4C) and apoptosis (Fig. 4D) in LPS-treated cells were counterbalanced after transfection of anti-miR-574-5p. Western blot further affirmed that protein level changes of Bcl-2, cleaved caspase 3 and cleaved PARP induced by si-circ_0001498#1 were reversed by miR-574-5p inhibitor (Fig. 4E). Meanwhile, miR-574-5p downregulation abated si-circ_0001498#1-induced inhibition of inflammatory reaction (Fig. 4F). The regulatory role of circ_0001498 in LPS-induced cell injury was achieved by sponging miR-574-5p.

Circ_0001498 acted as a miR-574-5p sponge to regulate SOX6 expression

Starbase (http://starbase.sysu.edu.cn) analysis indicated that SOX6 with binding sites for miR-574-5p might be a downstream target (Fig. 5A). Dual-luciferase reporter assay revealed that miR-574-5p interacted with SOX6 3'UTR-WT to reduce luciferase activity but it did not influence luciferase activity of SOX6 3'UTR-MUT group (Fig. 5B). SOX6 protein and mRNA levels were evidently increased in serums from sepsis patients compared with healthy controls (Fig. 5C,D). There was a negative correlation ($r = -0.596$, $p < 0.001$) between miR-574-5p and SOX6 levels (Fig. 5E) but a positive relationship ($r = 0.636$, $p < 0.001$) between circ_0001498 and SOX6 levels (Fig. 5F). LPS treatment resulted in protein upregulation of SOX6 in WI-38 cells, relative to control group (Fig. 5G). Western blot showed that SOX6 protein expression was inhibited after miR-574-5p overexpression,

and miR-574-5p inhibitor elevated SOX6 protein level (Fig. 5H). Moreover, anti-miR-574-5p transfection eliminated si-circ_0001498#1-mediated SOX6 protein downregulation in LPS-treated cells (Fig. 5I). Thus, circ_0001498 upregulated SOX6 by targeting miR-574-5p in LPS-treated WI-38 cells.

MiR-574-5p/SOX6 axis mitigated LPS-induced WI-38 cell injury

SOX6 protein level was much higher in SOX6 group compared with vector group (Fig. 6A), and SOX6 transfection recovered miR-574-5p-induced downregulation of SOX6 protein expression in LPS-treated WI-38 cells (Fig. 6B). Overexpression of miR-574-5p enhanced cell viability (Fig. 6C) and reduced cell apoptosis (Fig. 6D,E) after LPS treatment in WI-38 cells, then these impacts were countervailed by introduction of SOX6. TNF-α, IL-β and IL-6 concentration detection demonstrated that SOX6 upregulation attenuated the inhibitory effect of miR-574-5p on inflammatory response in LPS-treated WI-38 cells (Fig. 6F). All in all, miR-574-5p lightened LPS-induced cell damages by downregulating SOX6.

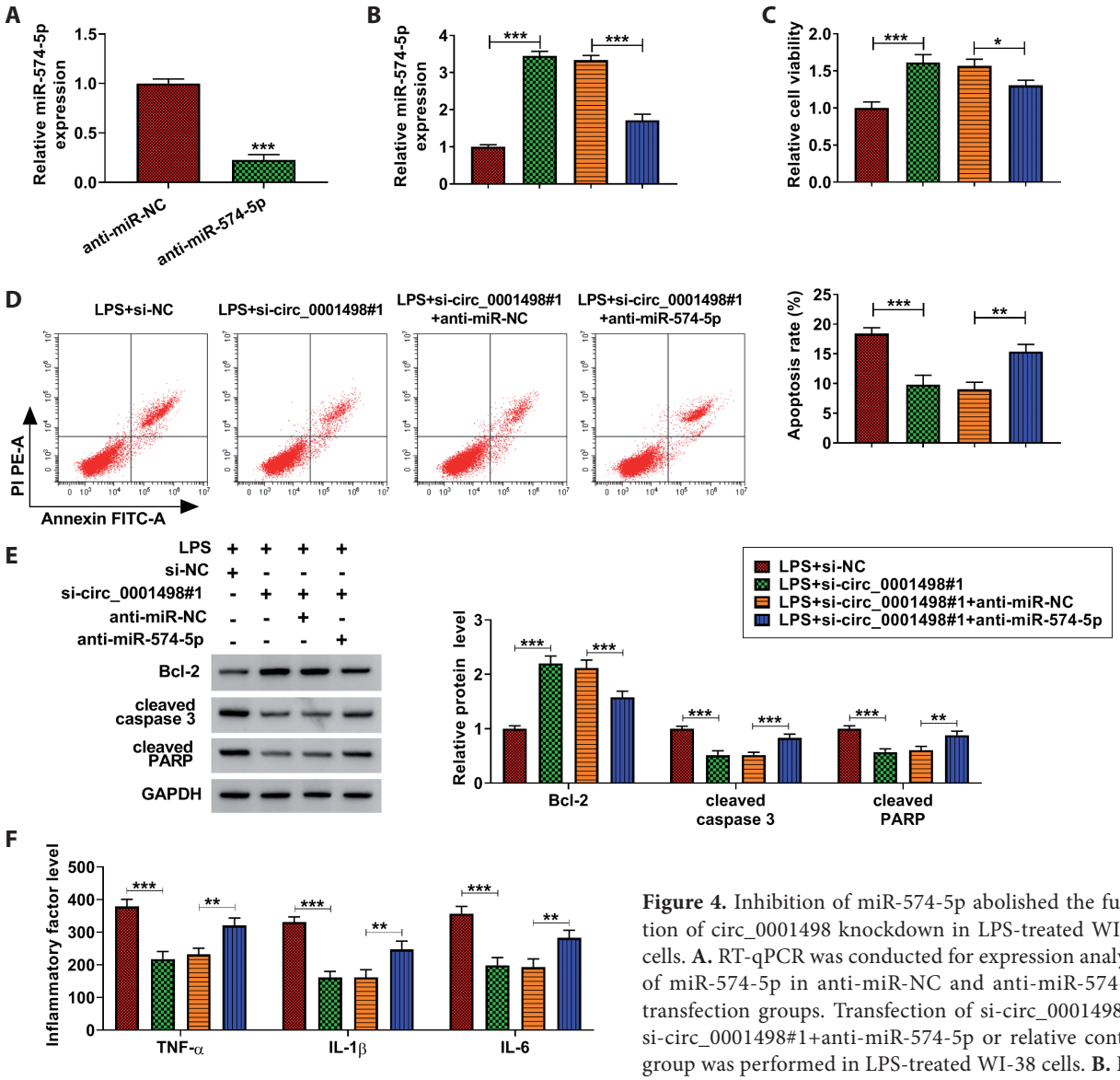

Figure 4. Inhibition of miR-574-5p abolished the function of circ_0001498 knockdown in LPS-treated WI-38 cells. **A.** RT-qPCR was conducted for expression analysis of miR-574-5p in anti-miR-NC and anti-miR-574-5p transfection groups. Transfection of si-circ_0001498#1, si-circ_0001498#1+anti-miR-574-5p or relative control group was performed in LPS-treated WI-38 cells. **B.** RT-qPCR was performed to examine miR-574-5p expression. **C.** CCK-8 assay was implemented to analyze cell viability. Flow cytometry (**D**) and Western blot (**E**) were carried out to assess cell apoptosis. **F.** ELISA was administrated to determine inflammatory cytokines. * $p < 0.05$, ** $p < 0.01$, *** $p < 0.001$.

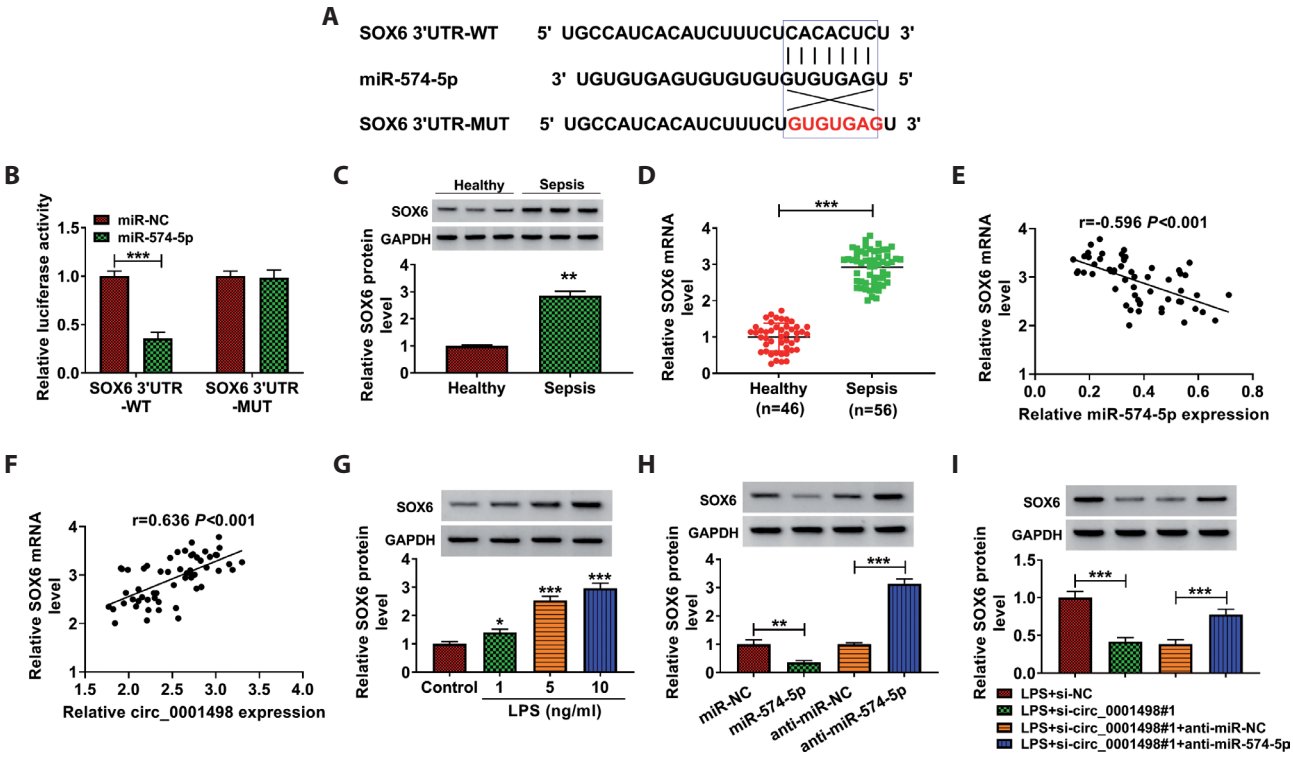

Figure 5. Circ_0001498 acted as a miR-574-5p sponge to regulate SOX6 expression. **A.** SOX6 3'UTR and miR-574-5p binding sites in starbase. **B.** SOX6 and miR-574-5p interaction was affirmed through dual-luciferase reporter assay. Western blot (**C**) and RT-qPCR (**D**) were used for mRNA dan protein detection of SOX6 in serums of sepsis patients and healthy controls. Pearson's correlation coefficient was used for linear analysis between SOX6 and miR-574-5p (**E**) or circ_0001498 (**F**). **G.** SOX6 protein expression was measured *via* Western blot after LPS treatment in WI-38 cells. **H.** The effects of miR-574-5p and anti-miR-574-5p on SOX6 protein level were analyzed using Western blot. **I.** The protein determination of SOX6 was carried out through Western blot in LPS+si-NC, LPS+si-circ_0001498#1, LPS+si-circ_0001498#1+anti-miR-NC and LPS+si-circ_0001498#1+anti-miR-574-5p groups. * $p < 0.05$, ** $p < 0.01$, *** $p < 0.001$.

Discussion

This study unraveled that circ_0001498 upregulated SOX6 through competitively binding to miR-574-5p, thereby involving in LPS-induced lung cell apoptosis and inflammation in sepsis-related ALI.

A handful of circRNAs are associated with sepsis-induced organ injury. For instance, circVMA21 alleviated sepsis-induced inflammatory reaction and oxidative stress in kidney (Shi et al. 2020). High level of circHIPK3 contributed to homeostasis and repair of intestinal epithelium in sepsis-induced acute injury (Xiao et al. 2021). Also, circ-Fryl overexpression accelerated cell autophagy to prevent sepsis-induced apoptosis and inflammation in ALI (Shen et al. 2021). Zou et al. (2020) identified that circ_0001679 and circ_0001212 increased apoptotic lung cells after LPS-induced sepsis. Herein, circ_0001498 level upregulation was detected in sepsis-related ALI patients. LPS has been used to establish sepsis-induced ALI cell model (Ren et al. 2021; Wang Y et al. 2021). Also, our experimental results demonstrated that cell viability was suppressed but apoptosis and inflammatory factors were stimulated by LPS in WI-38 cells. This study found that circ_0001498 was upregulated in sepsis samples compared to healthy controls. Further analysis exhibited that circ_0001498 knockdown by siRNA transfection has weakened LPS-induced cell injury, indicating the promoting effect of circ_0001498 in sepsis-associated ALI progression.

CircRNA/miRNA interaction axis is closely related to sepsis-induced complications. Li et al. (2012) declared that circVMA21 suppressed LPS-aroused cell inflammation and apoptosis in acute kidney injury by absorbing miR-199-5p. Wei et al. (2012) discovered that circ_0068888 protected renal tubular cells from LPS-induced oxidative injury and inflammatory response through targeting miR-21-5p. CircC3P1 reduced production of inflammatory cytokines in LPS-induced ALI *via* sponging miR-21 (Jiang et al. 2020). The current data validated circ_0001498/miR-574-5p target interaction and the reverted assays

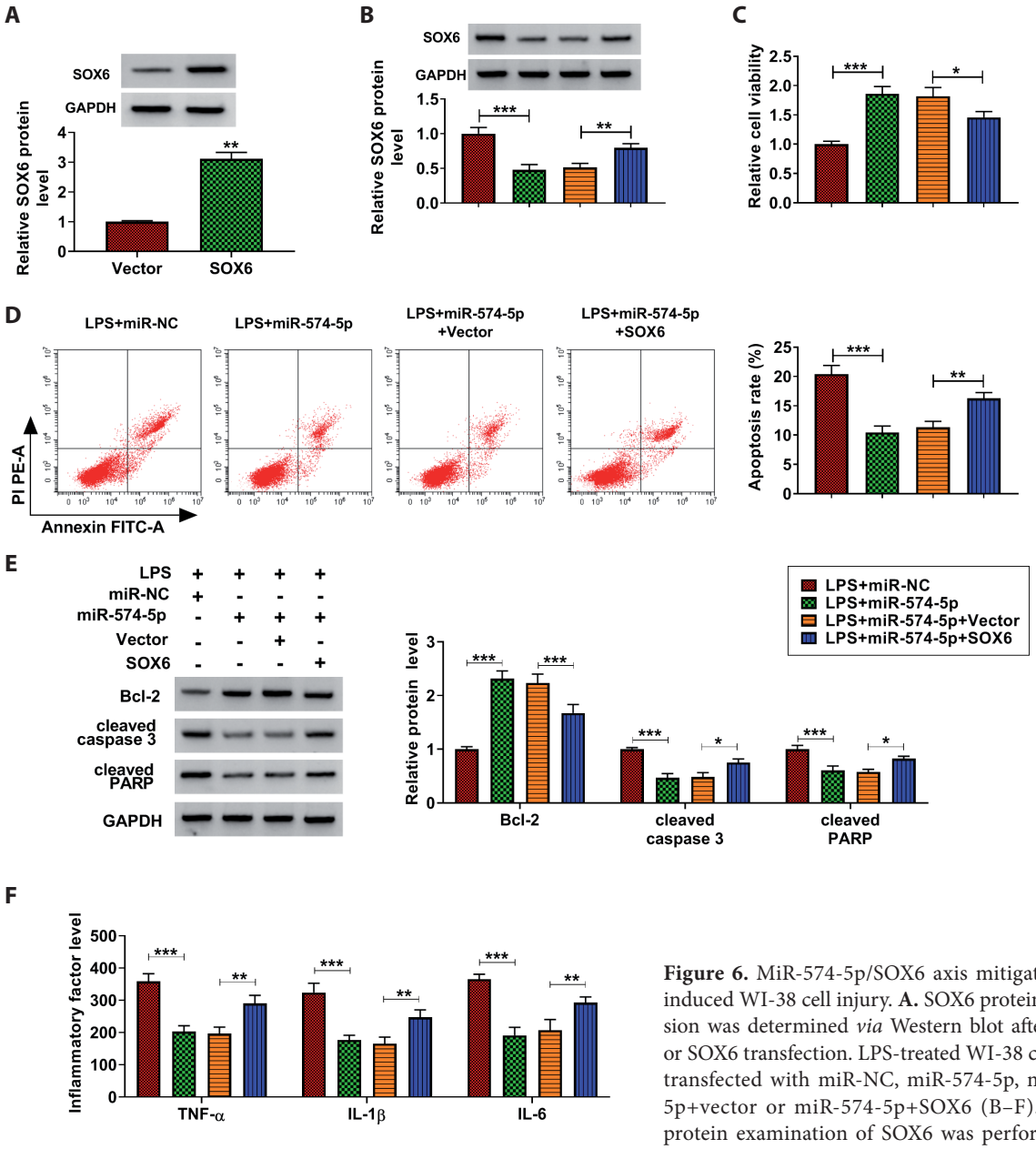

Figure 6. MiR-574-5p/SOX6 axis mitigated LPS-induced WI-38 cell injury. **A.** SOX6 protein expression was determined *via* Western blot after vector or SOX6 transfection. LPS-treated WI-38 cells were transfected with miR-NC, miR-574-5p, miR-574-5p+vector or miR-574-5p+SOX6 (B–F). **B.** The protein examination of SOX6 was performed *via* Western blot. **C.** CCK-8 assay was used for viability detection. Cell apoptosis was evaluated by flow cytometry (**D**) and Western blot (**E**). **F.** Inflammatory reaction was assessed *via* ELISA. * $p < 0.05$, ** $p < 0.01$, *** $p < 0.001$.

manifested that circ_0001498 regulation in LPS-caused lung cell injury was partly ascribed to act as a miR-574-5p sponge.

Many miRNAs can affect ALI progression induced by sepsis *via* regulating downstream targets. Overexpression of miR-129-5p attenuated sepsis-evoked ALI through reducing HMGB1 level (Yang et al. 2020), and miR-1398-5p prevented septic lung inflammation by downregulating SOCS6 (Ma et al. 2021). In this study, miR-574-5p targeted SOX6 and LPS-mediated cell injury was reversed by miR-574-5p *via* inhibiting SOX6 expression. CircRNA/miRNA/mRNA axis has been reported in acute injury induced by sepsis. For example, circTLK1 facilitated cell inflammation and oxidative stress in LPS-treated HK-2 cells to accelerate sepsis-related acute kidney injury (Xu P et al. 2021). The regulation of circ-Fryl in sepsis-induced ALI was achieved by targeting miR-490-3p/SIRT3 axis (Shen et al. 2021). Our expression analysis revealed that circ_0001498 upregulated

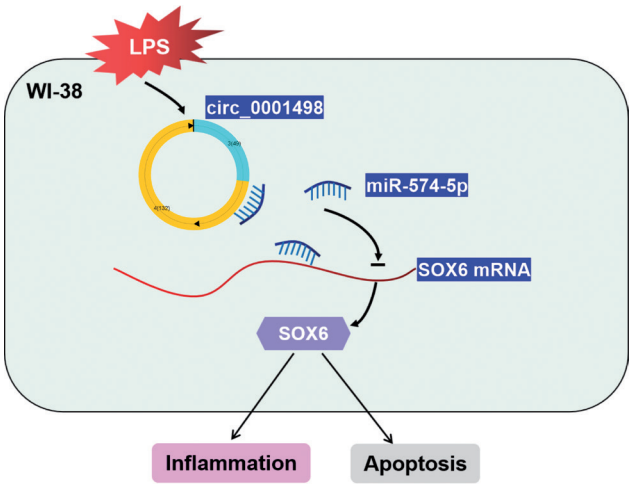

Figure 7. Circ_0001498/miR-574-5p/SOX6 axis participated in LPS-induced WI-38 cell inflammation and apoptosis.

SOX6 level by controlling miR-574-5p expression, suggesting that circ_0001498/miR-574-5p/SOX6 interaction network was implicated in sepsis-induced ALI progression in cell model.

Conclusion

In conclusion, circ_0001498 interacted with miR-574-5p to upregulate SOX6 expression to promote LPS-caused cell inflammation and apoptosis in WI-38 cells (Fig. 7). Circ_0001498 functioned as a pathogenic RNA by targeting miR-574-5p/SOX6 axis in sepsis-associate ALI.

Conflict of interest. The authors report no declarations of interest.

References

Beltran-Garcia J, Osca-Verdegal R, Nacher-Sendra E, Pallardo FV, Garcia-Gimenez JL (2020): Circular RNAs in sepsis: Biogenesis, function, and clinical significance. Cells **9,** 1544 https://doi.org/10.3390/cells9061544

Brandenburger T, Salgado Somoza A, Devaux Y, Lorenzen JM (2018): Noncoding RNAs in acute kidney injury. Kidney Int. **94,** 870-881 https://doi.org/10.1016/j.kint.2018.06.033

Ghafouri-Fard S, Khoshbakht T, Hussen BM, Taheri M, Arefian N (2021): Regulatory role of non-coding RNAs on immune responses during sepsis. Front. Immunol. **12,** 798713 https://doi.org/10.3389/fimmu.2021.798713

Guo W, Wang Z, Wang S, Liao X, Qin T (2021): Transcriptome sequencing reveals differential expression of circRNAs in sepsis induced acute respiratory distress syndrome. Life Sci. **278,** 119566 https://doi.org/10.1016/j.lfs.2021.119566

Jiang WY, Ren J, Zhang XH, Lu ZL, Feng HJ, Yao XL, Li DH, Xiong R, Fan T, Geng Q (2020): CircC3P1 attenuated pro-inflammatory cytokine production and cell apoptosis in acute lung injury induced by sepsis through modulating miR-21. J. Cell. Mol. Med. **24,** 11221-11229 https://doi.org/10.1111/jcmm.15685

Lennon FE, Singleton PA (2011): Role of hyaluronan and hyaluronan-binding proteins in lung pathobiology. Am. J. Physiol. Lung Cell. Mol. Physiol. **301,** L137-147 https://doi.org/10.1152/ajplung.00071.2010

Li X, Li R, Gong Q, Shi D, Song L, Song Y (2021): Circular RNA circVMA21 ameliorates lipopolysaccharide (LPS)-induced acute kidney injury by targeting the miR-199a-5p/NRP1 axis in sepsis. Biochem. Biophys. Res. Commun. **548,** 174-181 https://doi.org/10.1016/j.bbrc.2021.02.028

Livak KJ, Schmittgen TD (2001): Analysis of relative gene expression data using real-time quantitative PCR and the 2(-Delta Delta C(T)) method. Methods **25,** 402-408 https://doi.org/10.1006/meth.2001.1262

Ma J, Xu LY, Sun QH, Wan XY, Bing L. (2021): Inhibition of miR-1298-5p attenuates sepsis lung injury by targeting SOCS6. Mol. Cell Biochem. **476,** 3745-3756 https://doi.org/10.1007/s11010-021-04170-w

Panda AC (2018): Circular RNAs act as miRNA sponges. Adv. Exp. Med. Biol. **1087,** 67-79 https://doi.org/10.1007/978-981-13-1426-1_6

Qu S, Yang X, Li X, Wang J, Gao Y, Shang R, Sun W, Dou K, Li H (2015): Circular RNA: A new star of noncoding RNAs. Cancer Lett. **365,** 141-148 https://doi.org/10.1016/j.canlet.2015.06.003

Ren H, Mu W, Xu Q (2021): miR-19a-3p inhibition alleviates sepsis-induced lung injury via enhancing USP13 expression. Acta Biochim. Pol. **68,** 201-206 https://doi.org/10.18388/abp.2020_5505

Sadowitz B, Roy S, Gatto LA, Habashi N, Nieman G (2011): Lung injury induced by sepsis: lessons learned from large animal models and future directions for treatment. Expert Rev. Anti. Infect. Ther. **9,** 1169-1178 https://doi.org/10.1586/eri.11.141

Shen W, Zhao X, Li S (2022): Exosomes derived from ADSCs attenuate sepsis-induced lung injury by delivery of circ-fryl and regulation of the miR-490-3p/SIRT3 pathway. Inflammation **45,** 331-342 https://doi.org/10.1007/s10753-021-01548-2

Shi Y, Sun CF, Ge WH, Du YP, Hu NB (2020): Circular RNA VMA21 ameliorates sepsis-associated acute kidney injury by regulating miR-9-3p/SMG1/inflammation axis and oxidative stress. J. Cell. Mol. Med. **24,** 11397-11408 https://doi.org/10.1111/jcmm.15741

Sun W, Li H, Gu J (2020): Up-regulation of microRNA-574 attenuates lipopolysaccharide- or cecal ligation and puncture-induced sepsis associated with acute lung injury. Cell Biochem. Funct. **38,** 847-858 https://doi.org/10.1002/cbf.3496

Wang W, Yang N, Wen R, Liu CF, Zhang TN (2021): Long noncoding RNA: Regulatory mechanisms and therapeutic potential in sepsis. Front. Cell. Infect. Microbiol. **11,** 563126

https://doi.org/10.3389/fcimb.2021.563126
Wang Y, Shi Y, Zhang X, Fu J, Chen F (2021): Overexpression of limb bud and heart alleviates sepsis-induced acute lung injury via inhibiting the NLRP3 inflammasome. Biomed. Res. Int. **2021,** 4084371
https://doi.org/10.1155/2021/4084371
Wei W, Yao Y, Bi H, Xu W, Gao Y (2021): Circular RNA circ_0068,888 protects against lipopolysaccharide-induced HK-2 cell injury via sponging microRNA-21-5p. Biochem. Biophys. Res. Commun. **540,** 1-7
https://doi.org/10.1016/j.bbrc.2020.12.018
Xiao L, Ma XX, Luo J, Chung HK, Kwon MS, Yu TX, Rao JN, Kozar R, Gorospe M, Wang JY (2021): Circular RNA CircHIPK3 promotes homeostasis of the intestinal epithelium by reducing microRNA 29b function. Gastroenterology **161,** 1303-1317
https://doi.org/10.1053/j.gastro.2021.05.060
Xu H, Qi Q, Yan X (2021): Myricetin ameliorates sepsis-associated acute lung injury in a murine sepsis model. Naunyn Schmiedebergs Arch. Pharmacol. **394,** 165-175
https://doi.org/10.1007/s00210-020-01880-8
Xu HP, Ma XY, Yang C (2021): Circular RNA TLK1 promotes sepsis-associated acute kidney injury by regulating inflammation and oxidative stress through miR-106a-5p/HMGB1 axis. Front. Mol. Biosci. **8,** 660269
https://doi.org/10.3389/fmolb.2021.660269
Yang P, Xiong W, Chen X, Liu J, Ye Z (2020): Overexpression of miR-129-5p mitigates sepsis-induced acute lung injury by targeting high mobility group box 1. J. Surg. Res. **256,** 23-30
https://doi.org/10.1016/j.jss.2020.05.101
Zhang W, Li J, Yao H, Li T (2021): Restoring microRNA-499-5p protects sepsis-induced lung injury mice via targeting Sox6. Nanoscale Res. Lett. **16,** 89
https://doi.org/10.1186/s11671-021-03534-x
Zhong JX, Kong YY, Luo RG, Xia GJ, He WX, Chen XZ, Tan WW, Chen QJ, Huang YY, Guan YX (2021): Circular RNA circ-ERBB2 promotes HER2-positive breast cancer progression and metastasis via sponging miR-136-5p and miR-198. J. Transl. Med. **19,** 455
https://doi.org/10.1186/s12967-021-03114-8
Zhou D, Lin X, Wang P, Yang Y, Zheng J, Zhou D (2021): Circular RNA circ_0001162 promotes cell proliferation and invasion of glioma via the miR-936/ERBB4 axis. Bioengineered **12,** 2106-2118
https://doi.org/10.1080/21655979.2021.1932221
Zou Z, Wang Q, Zhou M, Li W, Zheng Y, Li F, Zheng S, He Z (2020): Protective effects of P2X7R antagonist in sepsis-induced acute lung injury in mice via regulation of circ_0001679 and circ_0001212 and downstream Pln, Cdh2, and Nprl3 expression. J. Gene Med. **22,** e3261
https://doi.org/10.1002/jgm.3261

Received: July 17, 2022
Final version accepted: October 21, 2022